Quantum path distributions for high-order harmonics in rare gas atoms

Mette B. Gaarde[1] and Kenneth J. Schafer[1,2]

[1]*Department of Physics, Lund Institute of Technology, P.O. Box 118, S-22100 Lund, Sweden*
[2]*Department of Physics and Astronomy, Louisiana State University, Baton Rouge, Louisiana 70803-4001*

We present quantum path distributions of high-order harmonics produced by rare gas atoms interacting with an intense 810 nm laser field, obtained by numerical integration of the time-dependent Schrödinger equation within the single active electron approximation. We find that the distributions are sensitive to the atomic potentials, and differ from the distributions predicted by the strong field approximation. We demonstrate that these differences can lead to significant differences in the time-frequency behavior of the harmonics produced in a macroscopic nonlinear medium.

High-order harmonics generated in the interaction between rare gas atoms and intense laser pulses have the demonstrated potential to produce trains of attosecond pulses [1]. In analogy with laser mode locking, the combination of several phase-locked harmonics produces a train of subfemtosecond pulses. Phase locking between different harmonics is, however, not trivial to obtain since their time-frequency behavior is often complicated [2,3]. This behavior has its origin in both the strong field single atom dynamics and the macroscopic effects of propagation and phase matching in the nonlinear medium. The single atom dynamics is best understood in the adiabatic limit, in which the main features of the harmonic generation process are determined by the instantaneous intensity I of the driving laser. In this limit, the time evolution of the system is completely determined by the intensity variation of the laser pulse. An analysis of the time-dependent phase of the generated harmonics, which gives rise to both spectral broadening and frequency modulation, is then equivalent to an analysis in terms of an intensity-dependent phase $\Phi(I)$. Quantum calculations demonstrate that each harmonic is composed primarily of contributions from just a few quantum paths, labeled α_j, whose intensity dependent phase is approximately linear: $\Phi_j = -\alpha_j I$ [4–6]. Recent experimental progress means that it is now possible to identify these quantum paths and measure their phase behavior [7]. The values of the phase coefficients α_j and their relative weights w_j define the quantum path distribution (QPD) for a high-order harmonic. Knowledge of the precise QPDs is crucial for determining the conditions under which attosecond pulse trains can be produced [2].

In this paper, we present accurate calculations of the intensity dependent dipole moments of high-order harmonics produced by rare gas atoms interacting with an intense 810 nm laser field, obtained by numerical integration of the time-dependent Schrödinger equation (TDSE) within the single active electron (SAE) approximation [8,9]. We analyze these dipole moments in terms of their QPDs and present three dimensional plots of $\{\alpha_j, w_j\}$ versus intensity. We find qualitative differences between the distributions for the different atoms. For example, in argon the largest contribution to the QPD corresponds to a very slow phase variation with intensity (small α). In contrast to this, we find that for neon and helium the QPDs have several equally strong contributions

from paths with faster phase variations (larger α). We also compare our results to QPDs calculated in the strong field approximation (SFA) [10], where the quantum paths arise naturally as stationary points in the quasiclassical action. We find that there are often large differences between the quantum path weights predicted by the two models. As shown in [11,5], the different quantum paths give rise to very different spatiotemporal characteristics of the macroscopic harmonics. We demonstrate that the TDSE and the SFA, leading to different predictions for the QPD, can, therefore, differ significantly in their prediction for the time-frequency characteristics of the harmonics after propagation and phase matching in the nonlinear medium. In [11,12], where the spatiotemporal separation of the different quantum paths in argon was first demonstrated, dipole moments calculated with the TDSE were used to model the experimental results. The agreement between theory and experiment was excellent [13].

We begin by obtaining the time-dependent wave function by numerical integration of the TDSE within the SAE [8,9]. From this we can calculate the time-dependent dipole moment, and thereby the dipole radiation spectrum. To obtain the intensity dependence of the dipole moment for each harmonic q, $d_q(I)$, we perform many calculations of the dipole moment for each harmonic at (different) quasiconstant intensities.

We analyze the intensity dependent dipole moment in terms of its conjugate variable α,

$$D_q(\alpha, I_0) = \int d_q(I) \exp(i\alpha I) W(I - I_0) dI. \qquad (1)$$

Here $D_q(\alpha, I_0)$ represents the contribution from the phase component α over the range of intensities close to I_0, defined by the translating window function $W(I - I_0)$ [14]. In the semiclassical picture, the different phase coefficients α correspond to different trajectories of the electron wave packet, and the size of α is an approximate measure of the time the wave packet spends in the continuum [10]. We also compare the TDSE calculations to predictions of the SFA, which is the quantum mechanical formulation of the semiclassical model. We calculate intensity dependent dipole moments as described in detail in [10], using a hydrogenic ground state
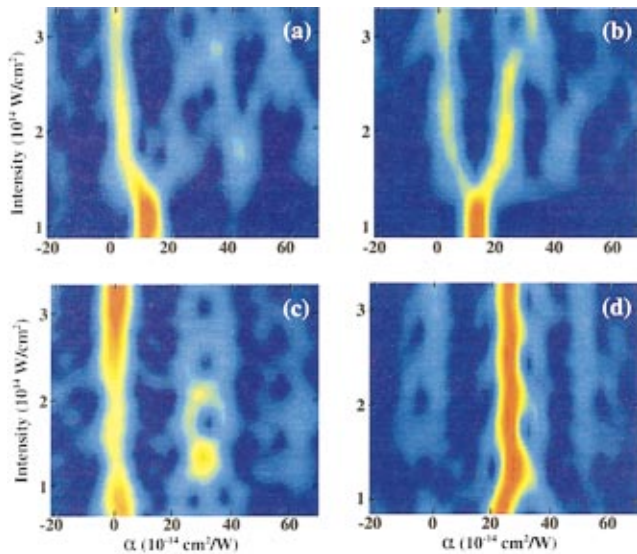
FIG. 1. (Color) Quantum path distributions for the 27th harmonic in argon, calculated with the TDSE (a) or the SFA (b), and for the 15th harmonic in argon calculated with the TDSE (c) or the SFA (d).

wave function and transition dipole matrix elements, which are scaled to model argon and neon.

In Fig. 1(a) we show the QPDs for the 27th harmonic in argon, calculated with the TDSE. For each intensity, the color scale shows the strength $|D_q(\alpha)|^2$ of the contributions from the different paths at that intensity. The weight w_j of a particular α_j can be found as the integrated strength over the vicinity of α_j. Many features from the semiclassical model can be recognized in the figure. At low intensity, when the 27th harmonic belongs to the cutoff region of the harmonic spectrum, there is only one phase component that contributes, i.e., there is only one important electronic trajectory. At higher intensities, when the harmonic belongs to the plateau region, the dipole moment always has several phase components, corresponding to several trajectories that the electron can follow and still return with the same kinetic energy. We find that it is the trajectory with the smallest α and the slowest phase dependence, $\alpha_1 \simeq 1$, that dominates (we give all α's in units of 10^{-14} cm^2/W). The trajectory with an α close to 40 is also prominant for a range of intensities, until it bifurcates into two contributions of which the smaller, $\alpha_3 \simeq 35$, is more prominent. We find this behavior to be typical for the high harmonics in argon.

In Fig. 1(b) we compare the result shown in (a) to the QPDs for the 27th harmonic obtained with the SFA. A corresponding comparison is shown for the 15th harmonic in argon in (c) and (d). Qualitatively, the agreement between the two models is good—they predict the existence of the same trajectories, and the same type of behavior as a function of the intensity. However, the quantitative agreement is poor. Whereas the TDSE predicts α_1 followed by α_3 to be the largest contributions, the SFA, in general, predicts the contribution of the second trajectory, $\alpha_2 \simeq 25$, to be the strongest.

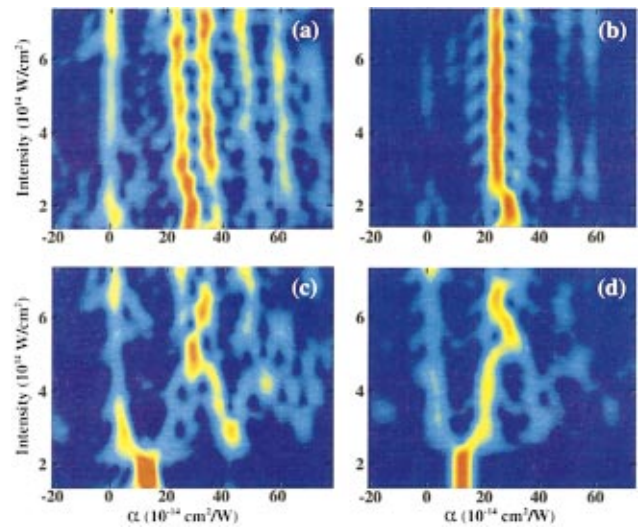Figure 2 demonstrates the species dependence of the

FIG. 2. (Color) Quantum path distributions for the 21st (a) and the 41st (c) harmonics in neon, calculated with the TDSE, and for the 21st (b) and the 41st (d) harmonics calculated with the SFA.

QPD, showing the 21st (a) and the 41st (c) harmonics in neon, generated with the TDSE. As is typical for the harmonics in neon, there are at least four α's that contribute almost equally to the dipole moment. The most important are $\alpha_1 \simeq 1$ and $\alpha_3 = 35$–40 at low intensities, and $\alpha_2 \simeq 25$ and $\alpha_3 \simeq 35$ at high intensities. This behavior is also typical for harmonics in helium. In contrast, the QPDs for harmonics in hydrogen (for which the ionization potential is similar to argon) behave much like that shown for argon in Fig. 1. In the SFA predictions for the 21st and 41st harmonics in neon, shown in (b) and (d), respectively, the α_2 contribution is again most prominent. For the 41st harmonic there is also a smaller contribution from α_1, whereas the α_3 contribution is weak. As is evident from the comparisons, the quantitative
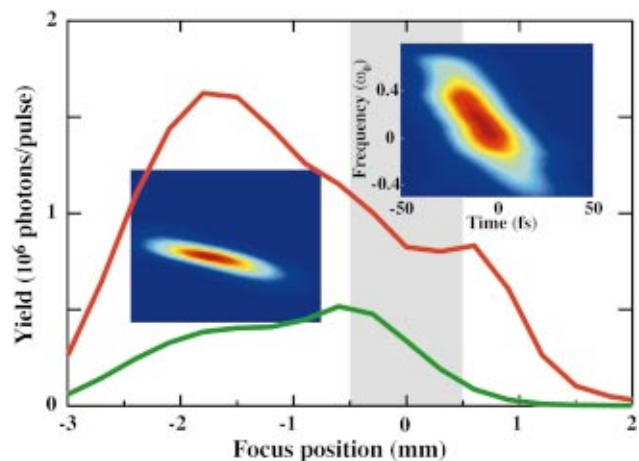

FIG. 3. (Color) Yield of the 27th harmonic in argon after propagation, as a function of the relative position of the focus and the center of the gas jet. When z_0 is negative, the focus is before the jet. Results using TDSE dipoles are shown with red line, SFA in green. Also shown are time-frequency representations of the harmonics for the focus positions $z_0 = -1.7$ mm and $z_0 = +0.6$ mm. The range of parameters is the same for both time-frequency plots.

differences between the TDSE and SFA are not intensity dependent, being equally large at low and high intensities.

The intensity dependence of the dipole phase is a direct result of the strong field electron dynamics leading to harmonic generation. Which trajectory dominates the emission process depends sensitively on the probability for tunneling, determined by the shape of the barrier, and on the amount of coherence the returning wave packet has with the ground state. Both of these are governed by the details of the atomic potentials, and we, therefore, find no generic rare gas atom QPD. In the SFA, the description of both the bound and continuum electron dynamics is highly simplified, which influences both the tunneling and the recombination processes. The disagreement between the TDSE and the SFA demonstrated in Figs. 1 and 2 is as one would expect—the weights of the different trajectories are wrong in the more approximate description.

We next examine the experimental consequences of the different QPDs predicted by the TDSE and the SFA by including effects of phase matching and propagation of the harmonics through a macroscopic nonlinear medium. We integrate the wave equation in three dimensions, within the paraxial and slowly varying envelope approximations [15]. We use the intensity dependent dipole moment as a source of the nonlinear part of the polarization field $P_q(r,z) = N(r,z)d_q(I(r,z))$, where $N(r,z)$ is the density of neutral atoms. These calculations take into account phase matching, absorption, dispersion, and effects of ionization, such as defocusing of the laser beam induced by the presence of free electrons and depletion of the neutral medium.

In Fig. 3 we show the yield of the 27th harmonic in argon after propagation through a 1 mm gas jet, as a function of the relative position of the laser focus and the center of the gas jet. The peak intensity is 2.5×10^{14} W/cm^2, the pulse length is 100 fs, and the confocal parameter $b=5$ mm. We show results of using both TDSE and SFA single atom dipoles. Apart from an overall discrepancy in the number of photons predicted by the two models, the shapes of the two curves also differ significantly. Whereas the TDSE dipole leads to a curve with two maxima, one on either side of the focus, the SFA curve has only one maximum, which is when the focus is close to (and before) the gas jet. The difference in the two shapes, and, in particular, the large difference between the results when $z_0=+0.6$ mm, can be understood in terms of the difference in the QPDs predicted by the two models. The insets show time-frequency representations of the propagated harmonic pulse (using TDSE dipoles) at the two optimal focus positions $z_0=-1.7$ mm (left) and $z_0=+0.6$ mm (right), calculated as described in [16]. When $z_0=+0.6$ mm, the harmonic has a large negative chirp. This is due to phase matching of the part of the dipole moment with $\alpha_3\approx40$. The SFA single-atom dipole moment, however, is so dominated by the contributions of $\alpha_2\approx25$ that this quantum path also governs the time-frequency behavior after phase matching. This leads both to a predicted chirp for $z_0=+0.6$ mm, which is only two thirds of that shown for the TDSE, and to the large difference in the yield between the
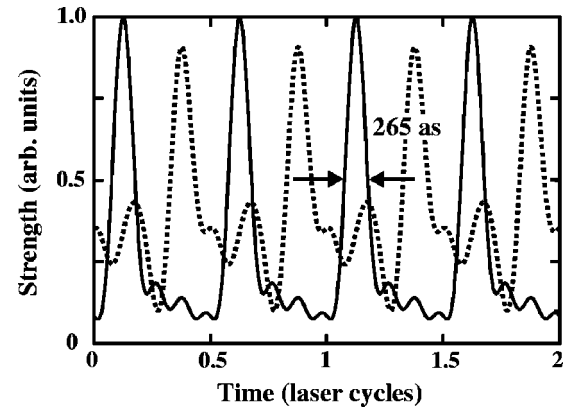

FIG. 4. Time profile of the combination of harmonics 15–23 in argon when the conditions for producing an attosecond pulse train are optimized (see text). TDSE result is shown with solid line, SFA result in dotted line.

two calculations. Note that the smaller SFA chirp also means that the SFA spectral bandwidth is much smaller than the TDSE bandwidth. The differences between the TDSE and the SFA results are, however, not uniform. For instance, at $z_0=-1.7$ mm, both models predict a small negative chirp like that shown in the figure.

Finally, in Fig. 4 we show the subcycle time profile of the harmonics 15–23 in argon, close to the peak of a 50 fs driving laser pulse with a peak intensity of 2.4×10^{14} W/cm^2. The phase-matching configuration has been chosen to optimize the production of a train of attosecond pulses by using a genetic algorithm to search through the parameter space of the propagation calculations using the TDSE dipoles (see [17]). The time profile (solid line) presents a nice train of pulses, one every half cycle of the laser field, each with a width of 265 as (1 as$=10^{-18}$ s). This is very similar to the results in [1] where a train of attosecond pulses with widths of 250 as was produced experimentally by combining the harmonics 11–19 in argon. The configuration used in Fig. 4 corresponds to good phase matching of the α_1 part of the dipole moment, which means that the harmonics have narrow spectral profiles and good temporal coherence properties. In contrast, the time profile predicted by the SFA in the same conditions (dotted line, scaled up by a factor of 15) has two pulses per half cycle and a much larger background. Since there is relatively less of the α_1 contribution and more of the α_2 contribution in the SFA single-atom QPD, the harmonics after propagation have much larger contributions from α_2 than for the TDSE result, which gives rise to the extra peaks and the increased background in the time profile.

In summary, we have shown that the QPDs for harmonics produced in rare gas atoms have significant differences between them. This means that the atomic structure has a direct influence on the behavior of the harmonics produced by an intense laser field, through the intensity dependence of the single atom phase. We found that the quantitative agreement between the QPDs from the TDSE and the SFA is often poor, since the description of the atomic interactions is highly sim-

plified in the SFA. We also demonstrated that these differences can lead to large discrepancies in the predictions for the time-frequency characteristics of the harmonics generated in a macroscopic nonlinear medium. Accurate calculations of the high harmonic QPDs are, therefore, necessary in order to make precise predictions of the macroscopic conditions under which attosecond pulses can be obtained.

[1] P.M. Paul *et al.*, Science **292**, 1689 (2001).

[2] Ph. Antoine, A. L'Huillier, and M. Lewenstein, Phys. Rev. Lett. **77**, 1234 (1996).

[3] Ph. Balcou *et al.*, J. Phys. B **32**, 2973 (1999).

[4] M. Lewenstein, P. Salières, and A. L'Huillier, Phys. Rev. A **52**, 4747 (1995).

[5] M.B. Gaarde *et al.*, Phys. Rev. A **59**, 1367 (1999).

[6] R. Kopold, W. Becker, and M. Kleber, Opt. Commun. **179**, 39 (2000).

[7] P. Salières *et al.*, Science **292**, 902 (2001).

[8] K.C. Kulander, K.J. Schafer, and J.L. Krause, in *Atoms in Intense Laser Fields*, edited by M. Gavrila (Academic Press, San Diego, 1992).

[9] K.J. Schafer and K.C. Kulander, Phys. Rev. Lett. **78**, 638 (1997).

[10] M. Lewenstein *et al.*, Phys. Rev. A **49**, 2117 (1994).

[11] M. Bellini *et al.*, Phys. Rev. Lett. **81**, 297 (1998).

[12] C. Lyngå *et al.*, Phys. Rev. A **60**, 4823 (1999).

[13] In contrast, it was not possible to reproduce the experimental result using dipole moments calculated with the SFA.

[14] Exactly as in [3], we analyze the intensity-dependent dipole phase only, letting $d_q(I)$ be constant. $W(I-I_0)$ is an asymmetric translating window function, also as described in [3].

[15] A. L'Huillier *et al.*, Phys. Rev. A **46**, 2778 (1992).

[16] M.B. Gaarde, Opt. Express **8**, 529 (2001).

[17] L. Roos, M. B. Gaarde, and A. L'Huillier, J. Phys. B **34**, 5041 (2001).